International Journal of Environmental Impacts
https://www.acadlore.com/journals/IJEI

Modeling the Distribution of Air Pollutants Around the Shipbuilding Industry: A Case Study of Batam City, Indonesia

Anita Pramawati[1,2*], Bintal Amin[3], Agrina Agrina[4], Budijono Budijono[5]

[1] Department of Environmental Science, Postgraduate Program, Universitas Riau, 28293 Pekanbaru, Indonesia
[2] Department of Health Sciences, Universitas Ibnu Sina, 29432 Batam, Indonesia
[3] Department of Marine Science, Faculty of Fisheries on Marine Science, Universitas Riau, 282931 Pekanbaru, Indonesia
[4] Department of Nursing, Faculty of Nursing, Universitas Riau, 28293 Pekanbaru, Indonesia
[5] Department of Aquatic Resources Management, Faculty of Fisheries and Marine Science, Universitas Riau, 282931 Pekanbaru, Indonesia

[*] Correspondence: Anita Pramawati (anitapramawati@uis.ac.id)

Received: 09-16-2025 **Revised:** 12-10-2025 **Accepted:** 02-09-2026

Citation: A. Pramawati, B. Amin, A. Agrina, and B. Budijono, "Modeling the distribution of air pollutants around the shipbuilding industry: A case study of Batam City, Indonesia," *Int. J. Environ. Impacts.*, vol. 9, no. 3, pp. 798–817, 2026. https://doi.org/10.56578/ijei090314.

Abstract: The expansion of the shipbuilding industry in coastal areas contributes substantially to economic development while simultaneously posing significant risks to air quality and community health. This study analyzed the concentration and spatial distribution of air pollutants and assessed non-carcinogenic health risks in the shipyard industrial area of Batam City. Air quality measurements were conducted for $PM_{2.5}$, SO_2, NO_2, CO, and Pb parameters at multiple receptor points at different distances from the emission source. The field measurement data were then integrated with dispersion modeling using the American Meteorological Society/Environmental Protection Agency Regulatory Model (AERMOD) based on local meteorological conditions. Health risk was evaluated using the Hazard Quotient (HQ) approach with reference to national air quality standards. Pollutant concentrations decreased consistently with increasing distance from emission sources, with $PM_{2.5}$ exhibiting the widest and most persistent spatial distribution. Although most pollutant concentrations remained below regulatory thresholds, $PM_{2.5}$ yielded HQ values exceeding 1.0 across all receptor distances up to 2000 m, indicating significant non-carcinogenic health risk at all observed distances. Model validation demonstrated strong spatial agreement between measured and simulated concentrations ($R^2 > 0.84$), with a consistent tendency toward underestimation of absolute values. The integration of spatial dispersion modeling with health risk assessment offers a comprehensive analytical framework for air quality management and public health protection in coastal industrial settings.

Keywords: Air quality; Shipyard; Tanjung Uncang; Batam City; Air pollution

1 Introduction

Industrial development is one of the main drivers of economic growth in many countries, including Indonesia. One of the sectors that is experiencing rapid growth is the shipbuilding industry, which has a strategic role in supporting maritime activities, international trade, and national defense [1]. Although the development of the shipyard industry contributes to improving the welfare of the community, this industrial activity also has various negative impacts, especially for people living around industrial estates. This impact is mainly related to the decline in air quality due to the production process, which has the potential to endanger human health and increase the risk of various diseases [2].

Air pollution from industrial activities can cause a wide range of health problems, including respiratory, cardiovascular, and nervous system disorders. In addition, air pollution also has a negative impact on the environment through a decrease in soil and water quality and vegetation damage [3]. Exposure to dust particles inhaled through the respiratory tract can trigger the body's defense mechanisms, such as coughing, sneezing, mucociliary disorders, and airway obstruction. If exposure occurs in large amounts and exceeds the threshold value, the condition can lead to a significant decline in lung function. According to a study [4], air pollution is one of the major risk factors for non-communicable diseases, including heart disease, stroke, chronic obstructive pulmonary disease, and lung cancer.

In response to these health risks, the Batam City Government stipulated Regional Regulation Number 4 of 2016, which prohibits the use of silica sand in the sandblasting process in open spaces. This policy aims to reduce exposure to silica dust that can cause lung disorders in the long term. Batam City, especially Tanjung Uncang Village, is one of the areas with the largest concentration of the shipbuilding industry in Indonesia. Industrial activities in this region include the construction, maintenance, and repair of ships involving sandblasting, welding, painting, and the use of various materials and chemicals, which produce air emissions in the form of $PM_{2.5}$, SO_2, NO_2, CO, and heavy metals such as Pb [5].

Sandblasting is one of the main activities in the shipbuilding industry, involving the use of silica sand or other abrasive materials to clean and prepare metal surfaces. This process generates $PM_{2.5}$ that poses occupational health risks, particularly when conducted in open or poorly controlled environments. Previous studies have reported that shipyard operations contribute to increased occupational exposure to $PM_{2.5}$ among workers [6]. In urban coastal areas, pollutant dispersion becomes more complex due to the influence of wind speed and direction, requiring a modeling approach capable of accurately representing the spatial distribution of pollutants.Although the shipbuilding industry has a positive economic impact, the air pollution it produces poses a serious challenge to public health. $PM_{2.5}$ is able to penetrate the alveoli of the lungs and enter the bloodstream, causing inflammation and decreased lung function. SO_2 and NO_2 gases can irritate the respiratory tract, while heavy metals such as Pb have an impact on the central nervous system, especially in children. In addition, CO interferes with the process of oxygen transport in the blood, while low levels of O_2 in the air reflect a decrease in air quality [3]. This impact is exacerbated by seasonal wind patterns that have the potential to bring industrial pollutants to residential areas, as reflected in the high cases of respiratory infections in the area around industrial areas.

Various previous studies have conducted air quality mapping in urban and industrial areas using spatial analysis approaches. Geographic information systems (GIS), land-use regression, and spatial modeling methods have been widely applied to analyze the distribution and spatial variation of air pollutants such as PM_{10}, SO_2, NO_2, and CO in relation to emission sources and surrounding environmental conditions [7, 8]. Previous studies have also reported that shipyard operations contribute to increased occupational exposure to $PM_{2.5}$ among workers [6]. In addition, open abrasive blasting activities can generate hazardous airborne particulate emissions that may be transported by wind to nearby residential areas; however, studies integrating pollutant dispersion mapping with spatial technology in shipyard environments remain limited [9].

In general, previous studies have tended to analyze pollutant concentrations and their health impacts separately, and have not applied the comprehensive spatial approach recommended by the United States Environmental Protection Agency (U.S. EPA) for the simulation and prediction of pollutant dispersion based on wind direction. In fact, an integrated spatial approach is essential for accurately visualizing the distribution of pollutants, identifying areas with the highest levels of exposure, and bridging technical analysis of air quality with public health risk evaluation. Therefore, an analytical framework is needed that is able to integrate pollutant dispersion modeling with health risk assessment to provide a more comprehensive understanding of the impact of air pollution in coastal industrial areas.

Overall, previous research has largely focused on the analysis of pollutant concentrations and their associated health impacts, often treating air quality assessments and health risk evaluations as separate analytical components. In addition, comprehensive spatial approaches recommended by regulatory agencies such as the U.S. EPA to simulate and predict the spread of pollutants based on wind direction have not been consistently applied. As a result, the spatial relationship between pollutant distribution patterns and the level of health risks in coastal shipbuilding industrial areas has not been adequately examined. Therefore, a more integrated spatial approach is needed to accurately visualize pollutant dispersion, assess exposure gradients, and identify high-risk zones. In response to this research gap, this study offers novelty through the application of an integrated analysis framework that combines spatial mapping of air quality concentration and distribution based on multi-pollutant dispersion modeling ($PM_{2.5}$, SO_2, NO_2, CO, Pb, and O_2) with health risk assessment using the Hazard Quotient (HQ) approach and risk mapping. Unlike previous studies that typically analyze air quality conditions and health impacts in isolation, this study simultaneously linked the spatial distribution of pollutants to the level of health risks associated with inhalation, allowing the identification of high-risk zones in coastal urban shipbuilding industrial estates. Methodologically, multi-point field measurement data was integrated with the output of the American Meteorological Society/Environmental Protection Agency Regulatory Model (AERMOD) dispersion model to map pollutant distribution patterns based on wind direction and area characteristics. These findings suggest that certain pollutants—particularly $PM_{2.5}$, NO_2, and Pb—contribute predominantly to increased health risks, while exposure levels and associated risks systematically decrease with increasing distances from emission sources. By moving beyond the purely technical evaluation of pollutant concentrations, this integrated approach provides a more comprehensive understanding of the relationship between the distribution of pollutants and health risks and can serve as an analytical framework for similar studies in coastal industrial areas with comparable characteristics. In particular, the spatial-health risk relationship identified in this study provides applied insights into exposure patterns at the industrial-residential interface, which is relevant to other coastal shipbuilding and heavy industrial areas characterized by open process activities and proximity to

surrounding settlements.

Comparative analysis across pollutant types highlights the characteristics of the different spatial dispersions between particulate and gaseous emissions. $PM_{2.5}$ and NO_2 exhibit wider and more persistent exposure zones than SO_2 and CO, reflecting their emission sources and atmospheric behavior in coastal industrial environments. $PM_{2.5}$, which is mainly derived from sandblasting and combustion processes, exhibits limited dispersion and prolonged suspension in the atmosphere, while CO exhibits relatively rapid dilution, resulting in lower spatial exposure intensities. This contrast underscores that pollutant concentrations alone do not fully represent environmental risks, as spatial distribution patterns and duration of exposure play an important role in determining health-related impacts.

2 Method

This research was conducted in Batam City, around the shipyard industrial area with sandblasting activities (Figure 1), from July to December 2024, with a research duration of three months. The test was conducted based on wind direction and modeling of the distribution of $PM_{2.5}$, SO_2, NO_2, CO, and Pb concentrations using AERMOD View software.

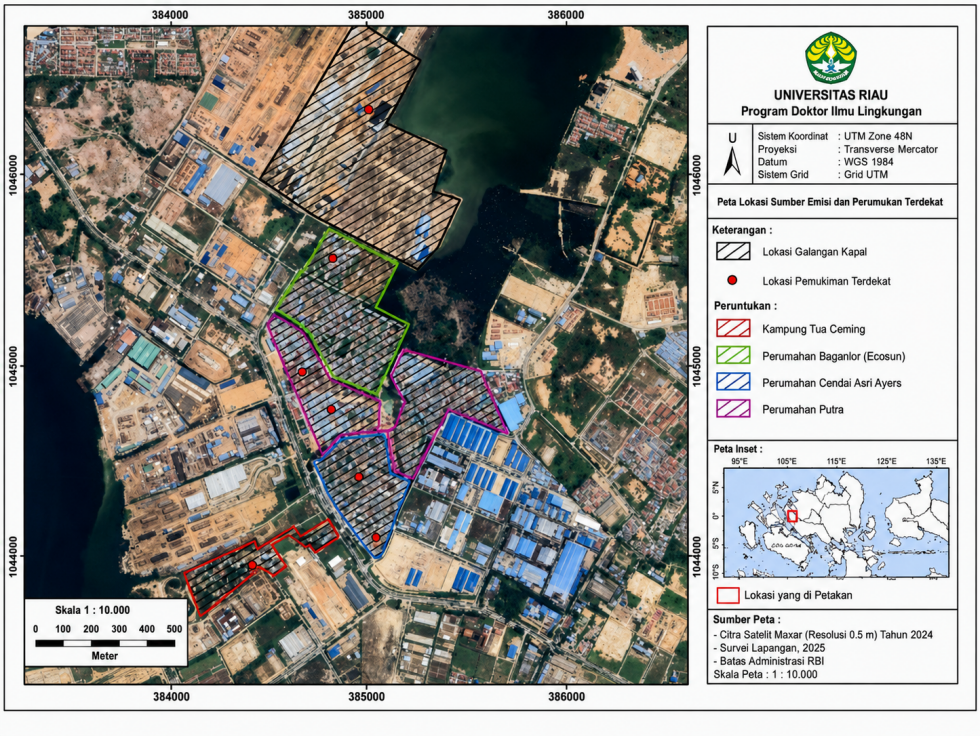

Figure 1. Receptor locations and segments

2.1 Material

The tool used for the measurement of pollutants $PM_{2.5}$, Low Volume Air Sampler Gent, Pb uses a High Volume Air Sampler device from the PM Sampler brand Laos. Gaseous pollutants, including SO_2, CO, and NO_2 in solution, were captured using an impinger/air sampling pump-type instrument from Sibata.

The location of the receptors used in this study represented several residential areas at different distances from the main emission source. The receptor point is selected based on its proximity to industrial activities and its position, which is spatially relevant to the direction of pollutant distribution. Table 1 presents the coordinates and distances of each settlement used as a monitoring point.

Table 1. Receptor location (settlement coordinate point)

No.	Information	Longitude (X)	Latitude (Y)	Distance (m)
1	Bagaman Citramas Housing	103.918621	1.070897	500
2	Scissors Old Village	103.918552	1.063909	1000
3	Pluto Housing	103.920678	1.057915	1500
4	Ayana Central Housing	103.914905	1.056549	2000

2.2 Research Procedure

The Low Volume Air Sampler was used as the $PM_{2.5}$ particle concentration measuring device. The Low Volume Air Sampler device was equipped with a 47 mm diameter filter, using a Teflon or quartz filter. The filter was pre-conditioned through the drying process and weighed first using an analytical scale. The tool was placed in a representative location at a height of 1.5–3 m above ground level. The airflow rate was set to about 16.7 L/min and allowed to suck in air for 24 hours. After the sampling period, the filter is removed, reconditioned, and reweighed. The $PM_{2.5}$ concentration was calculated based on the difference in filter mass before and after sampling, as well as the volume of filtered air, expressed in μg/Nm^3.

Monitoring of SO_2, NO_2, O_2, and CO gases using Sibata brand impinger pump/air sampling type tools: prepared an impinger containing reservoir solution according to the gas type: SO_2: a solution of hydrogen peroxide (H_2O_2) and NO_2 was used. NaOH + Na_2AsO_3 solution. CO: iodine pentoxide (I_2O_5) solution, or potassium iodide solution. The impinger was connected to an air pump (Sibata) and a flowmeter, and the flow rate was calibrated at a speed between 1 and 2 L/min. Sample collection: The tool was placed in a representative location, and the pump was turned on for 30 minutes to 1 hour. Make sure that the volume of the inhaled air was well measured (using a rotameter or flowmeter). The retaining solution was then stored in a dark bottle and labeled. SO_2 was analyzed using the pararosaniline method and measured using a spectrophotometer at a wavelength of 548 nm. NO_2 was analyzed using the Saltzman method and measured using a spectrophotometer at a wavelength of 540 nm. CO was analyzed using non-dispersive infrared (NDIR) or colorimetry methods, if available. The concentration was calculated based on the air volume of the sample and the amount of dissolved gases in the solution. The results were expressed in μg/Nm^3 or ppm, as per the requirements of the analysis.

2.3 Receptor Locations and Segments

This study uses several receptor points that represent residential areas around the research area. The location of the receptor is selected based on its distance from the emission source and its geographical position. Table 1 shows the coordinate and distance data of each settlement used as a receptor point.

2.4 Data Processing

Data processing was carried out to analyze the spatial distribution of $PM_{2.5}$, SO_2, NO_2, CO, and Pb concentrations using the AERMOD.

The model simulates the dispersion of pollutants by combining meteorological parameters, emission characteristics, and local topographic conditions. To evaluate the reliability of the results of the AERMOD simulation, statistical validation was carried out by comparing the modeled concentrations with field measurement data using the determination coefficient (R^2). R^2 indicates the proportion of variance in the observed data that can be explained by model simulations and is commonly used to assess the performance of air dispersion models in accordance with U.S. EPA guidelines.

R^2 is calculated using the following formula:

$$R^2 = 1 - \frac{\sum (O_i - P_i)^2}{\sum (O_i - \bar{O})^2}$$

where, O_i is the observed concentration obtained from field measurements, P_i is the concentration of pollutants predicted by the AERMOD model, and $\bar{O}$ is the average value of the observed concentration. An R^2 value of $\geq$0.7 indicates good model performance and an acceptable agreement between the simulated and observed data, in line with the U.S. EPA air quality modeling evaluation criteria.

In addition to the analysis of air quality concentrations, health risk assessments were carried out using the HQ approach to evaluate the risk of non-carcinogenic inhalation at each receptor site. The HQ value is calculated by comparing the observed pollutant concentration with the regulatory reference concentration based on Government Regulation No. 22 of 2021. For $PM_{2.5}$, the annual mean standard of 15 μg/Nm^3 as stipulated in PP No. 22 of 2021 Appendix VII was applied as the reference concentration for health risk classification, consistent with the measurement period of this study which represents an annual exposure estimate. For all other parameters (SO_2, NO_2, CO, and Pb), the corresponding national ambient air quality standards (Nilai Ambang Batas, NAB) values per PP No. 22 of 2021 were applied as reference concentrations for HQ calculation.

Furthermore, spatial risk mapping was performed by overlaying HQ values with pollutant dispersion maps to identify areas with elevated health risk. This integrated approach enables a more comprehensive assessment of population exposure across the study area.

Comparative analysis across pollutant types highlights the different spatial dispersion characteristics between particulate and gaseous emissions. $PM_{2.5}$ exhibits wider and more persistent exposure zones than SO_2, NO_2, and CO, reflecting its emission sources and atmospheric behavior in coastal industrial environments. $PM_{2.5}$, which is mainly

derived from sandblasting and combustion processes, demonstrates prolonged suspension in the atmosphere due to its fine particle size, whereas CO undergoes relatively rapid dilution, resulting in lower spatial exposure intensities. This contrast underscores that pollutant concentrations alone do not fully represent environmental risks, as spatial distribution patterns and duration of exposure play an equally important role in determining health-related impacts.

3 Results and Discussion

3.1 Model Validation Results for Multiple Pollutants

The model validation results for multiple pollutants are presented in Figure 2, which illustrates the measured air pollutant concentrations at varying distances from emission sources compared to the NAB. Based on the modeling results, emissions from the shipyard industrial source exerted varied effects on ambient concentration levels. The most significant contributions were observed for $PM_{2.5}$, which exhibited the highest concentrations across all receptor distances, particularly within a radius of 0–500 m from the emission source. Pb concentrations remained relatively constant across distances, reflecting the stable physicochemical characteristics of lead during atmospheric transport. In contrast, for SO_2, NO_2, and CO parameters, the contribution of industrial activities to ambient air quality was relatively minimal, with all values remaining well below the NAB as stipulated in PP No. 22 of 2021. Overall, total pollutant concentrations decreased consistently with increasing distance from the emission source, which reflects the effectiveness of natural atmospheric dispersion processes.

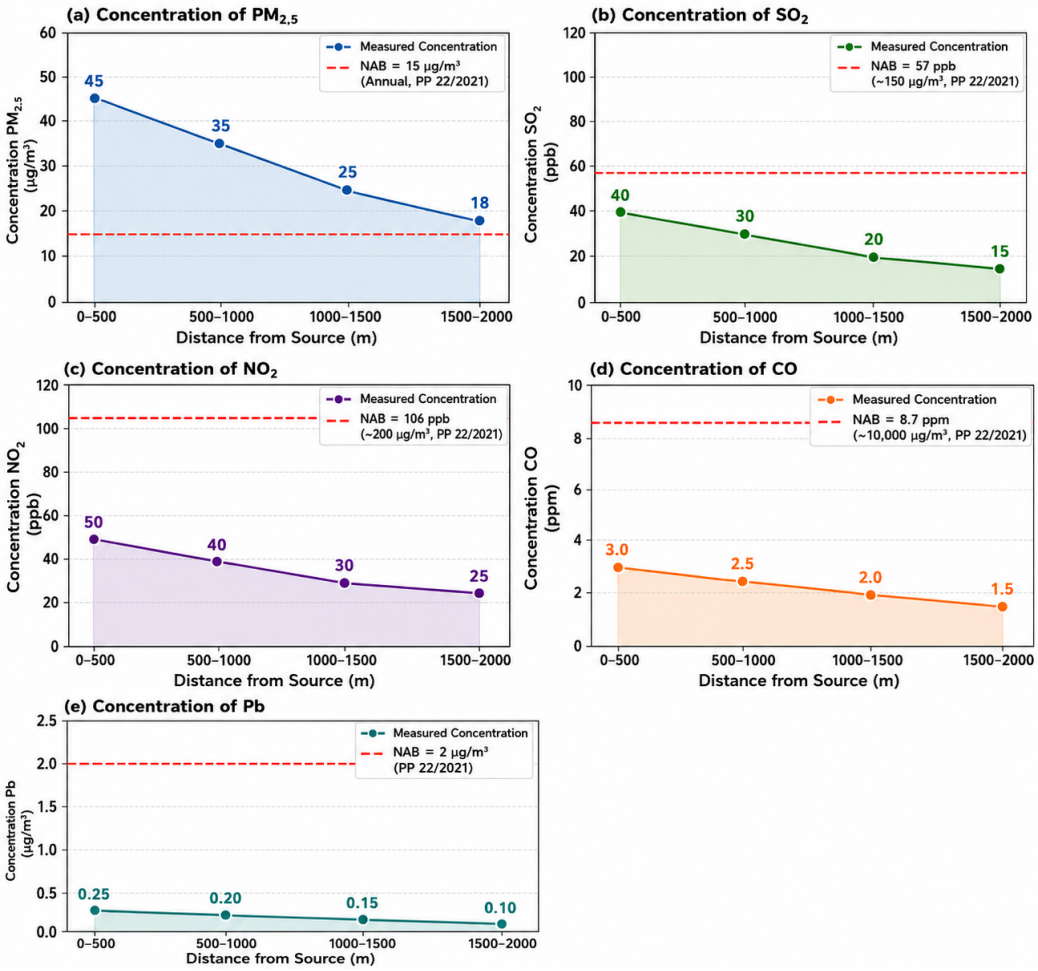

Figure 2. Measured air pollutant concentrations at varying distances from emission sources compared to national ambient air quality standards (Nilai Ambang Batas, NAB)

3.2 Air Quality Parameters

The measurement of air quality concentration is carried out based on the distance from the main emission sources in the shipyard industrial area. The parameters measured will include $PM_{2.5}$, SO_2, NO_2, CO, and Pb, and they with the threshold values set in Government Regulation No. 22 of 2021. The average concentrations of each parameter at various observation distances are listed in Table 2.

Table 2. The average value and its category for each parameter

Parameter (unit)	Distance (m)				NAB	Category
	0–500	500–1000	1000–1500	1500–2000		
PM2.5 (μg/m^3)	45	35	25	18	15	High
SO2 (ppb)	40	30	20	15	57	Safe
NO2 (ppb)	50	40	30	25	106	Safe
CO (ppm)	3	2.5	2	1.5	8.7	Safe
Pb (μg/m^3)	0.25	0.2	0.15	0.1	2	Safe

Note: NAB, national ambient air quality standards, Nilai Ambang Batas.

As shown in Figure 2 and Table 2, the highest $PM_{2.5}$ concentration was detected at a distance of 0–500 m of 45 μg/m^3, which gradually decreased to 18 μg/m^3 at a distance of 1500–2000 m. This value exceeds the annual NAB of 15 μg/m^3 (PP No. 22 of 2021), so it is categorized as high, indicating potential health hazards, especially for vulnerable groups. Furthermore, the SO_2 concentration was recorded at 40 ppb at the nearest distance and decreased to 15 ppb at the farthest distance. However, all of these values are below the NAB of 57 ppb (equivalent to 150 μg/m^3 per PP No. 22 of 2021); therefore, they are categorized as safe.

The decrease in the concentration of pollutants observed with increasing distances from emission sources shows a clear spatial gradient consistent with the theory of atmospheric dispersion. Pollutants emitted from shipyard activities show the highest concentrations in the range of nearby receptors (0–500 m) and are gradually reduced over longer distances due to dilution and dispersion by wind and atmospheric turbulence. Among the measured parameters, $PM_{2.5}$ showed the most prominent spatial persistence compared to gaseous pollutants, indicating higher accumulation potential in nearby residential areas. These findings suggest that differences in pollutant behavior are strongly influenced by their physical and chemical properties, especially particle size and atmospheric residence time, which regulate dispersion efficiency and exposure patterns around industrial sources.

3.3 Air Quality Distribution ($PM_{2.5}$, SO_2, NO_2, CO, Pb)

The distribution of air quality around the shipyard industrial area in Batam City used $PM_{2.5}$, SO_2, NO_2, CO, and Pb. Analysis was carried out using the spatial interpolation method based on direct concentration measurements in the field. These mapping results provide a visual overview of areas with different levels of pollutant exposure, allowing us to determine which locations have the highest concentrations of pollutants.

3.3.1 Concentration distribution modeling $PM_{2.5}$

Figure 3 shows the distribution of $PM_{2.5}$ concentrations in Batam City based on the results of spatial measurements and interpolation. This map shows the areas with the highest levels of exposure, which are generally around industrial areas. The results of the analysis of the spatial distribution of air quality in the area around the shipyard industry in Batam City. The parameters of the pollutants analyzed included $PM_{2.5}$, SO_2, NO_2, CO, and Pb.

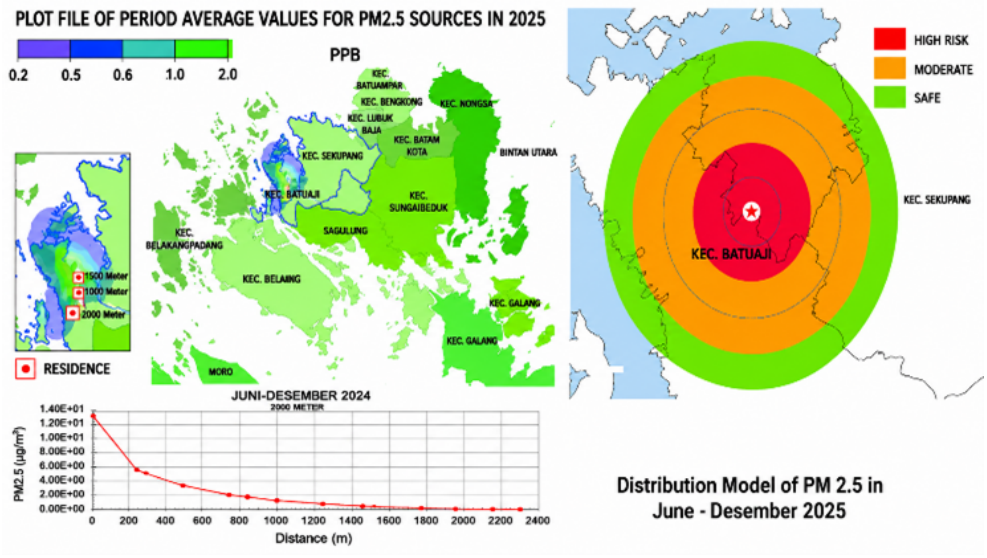

Figure 3. $PM_{2.5}$ concentration distribution modeling

Based on Figure 3, modeling the average distribution of $PM_{2.5}$ concentrations for the period July to December 2024 shows the spatial pattern of air pollution in the shipyard industrial area of Batam City. Based on the results of modeling using AERMOD, a maximum $PM_{2.5}$ concentration value of 2.16 $\mu g/m^3$ was obtained at coordinates 379885, 1186793, which is located in the center of shipbuilding industrial activities. The zone of high concentration (1.5–2.16 $\mu g/m^3$) is indicated by the red and orange colors that spread to a radius of ±500 m from the source. The further away from the emission point, $PM_{2.5}$ concentrations show a gradual decline, characterized by green gradations (0.5–1.0 $\mu g/m^3$) at a radius of 500–1000 m, and purple (<0.2 $\mu g/m^3$) at a radius of more than 1500 m. This pattern shows that $PM_{2.5}$ pollution is concentrated in industrial areas and spreads radially, following the dominant wind direction and local topographic conditions. On the map, four settlements were identified as being in the $PM_{2.5}$-exposed zone.

Settlements within a radius of 1000 m are in zones with $PM_{2.5}$ concentrations between 0.5–1.5 $\mu g/m^3$. Although this value is still relatively low based on national air quality standards, the presence of dense settlements near emission sources increases the population's vulnerability to long-term exposure, especially in at-risk groups such as children, the elderly, and people with respiratory diseases. Referring to Government Regulation Number 22 of 2021 concerning the Implementation of Environmental Protection and Management, the ambient air quality standard for $PM_{2.5}$ is set at 55 $\mu g/m^3$ for the daily average and 15 $\mu g/m^3$ for the annual average. Thus, the maximum value recorded in the modelling (2.16 $\mu g/m^3$) is still well below the permissible threshold, but referring to the environmental health literature and World Health Organization (WHO) recommendations [4], No level of $PM_{2.5}$ exposure is considered completely safe, as even long-term exposure to low concentrations can have significant health impacts. In addition to anthropogenic sources from industry, $PM_{2.5}$ also comes from transportation activities, fossil fuel burning, and household activities [10]. In shipyard industrial areas, such as Batam, sandblasting, painting, and burning diesel fuel on large engines are the main contributors.

According to a study [8], $PM_{2.5}$ is the most dangerous fraction of air particles due to its ability to penetrate deep into the respiratory system and reach the lung alveoli due to its complex chemical composition. Heavy metals, carbon black, and organic compounds make $PM_{2.5}$ toxic and contribute significantly to the global burden of disease, especially heart disease, stroke, and chronic lung disorders. Fine particles of $PM_{2.5}$ can enter the lung alveoli, triggering airway inflammation (bronchitis, asthma), decreased lung function, chronic obstructive pulmonary disease, cardiovascular disorders, and long-term carcinogenic potential [11].

Previous research has shown that people and workers living around industrial estates have a higher susceptibility to lung disorders. Studies [12, 13] have reported increased respiratory health risks associated with particulate air pollution exposure. Previous evidence has also demonstrated that long-term exposure to $PM_{2.5}$ is associated with impaired lung function and adverse respiratory outcomes [13]. The study found that bricklayers in Taktakan District, Serang, who were exposed to $PM_{2.5}$ experienced significant impaired lung function. Similar findings were reported by study [5] in the Gresik industrial area, where people living within a radius of 1 km from the cement industry showed an increase in the prevalence of respiratory disorders. Meanwhile, in China, it was reported that high $PM_{2.5}$ exposure in densely populated industrial areas was strongly correlated with increased hospitalizations due to chronic lung disease [14].

In contrast to these findings, this study shows that $PM_{2.5}$ concentrations around the shipyard industry are still relatively low, with a maximum value of 2.16 $\mu g/m^3$, well below the threshold and concentration reported in previous studies (above 15 $\mu g/m^3$). This shows that although shipbuilding industry activities contribute to $PM_{2.5}$ emissions, the scale has not yet reached the acute levels of pollution that occur in the petrochemical and brick industries. However, long-term exposure still needs to be monitored, given the cumulative nature of $PM_{2.5}$, which has a long-term impact on lung health. Although the modelling results show that the concentration of $PM_{2.5}$ around the shipyard industry is still below the national quality standard, and the existence of densely populated settlements within a radius of less than 1000 meters (Kampung Tua Cunting) requires special attention. These areas are inhabited by vulnerable groups, such as children, the elderly, and individuals with chronic diseases, who are more sensitive to exposure to pollutants.

The Spatial distribution of modeled air pollutant concentrations generated using the AERMOD dispersion model around the shipyard area (Figure 3). The contour map depicts high, medium, and low exposure zones, with the highest concentrations observed near industrial emission sources, gradually declining outward. Receptor points and surrounding residential areas are layered to visualize potential population exposure and risk zones. This integrated map supports the assessment of pollutant dispersion patterns influenced by meteorological characteristics and local land use.

3.3.2 Concentration distribution modeling SO_2

Figure 4 presents the spatial distribution of SO_2 concentrations in a more visual way, making it easier to identify the areas with the highest levels of exposure. This information is important for decision-making in air pollution control.

Figure 4 shows a map of the distribution of SO_2 concentrations, which is the result of modeling using internationally recognized AERMOD software to predict the dispersion of air pollutants. This map depicts the spatial distribution of SO_2 derived from shipyard industry activities in Batam City from June to December 2024. The SO_2 concentration in

the map is shown in parts per billion (ppb) with a color gradation depicting the intensity concentration from blue (lowest) to red (highest). The maximum concentration detected was 4.1×10^{-3} ppb, located at coordinates 379393.27 (X), 119173.36 (Y). This point is located less than 500 m from the center of industrial activity.

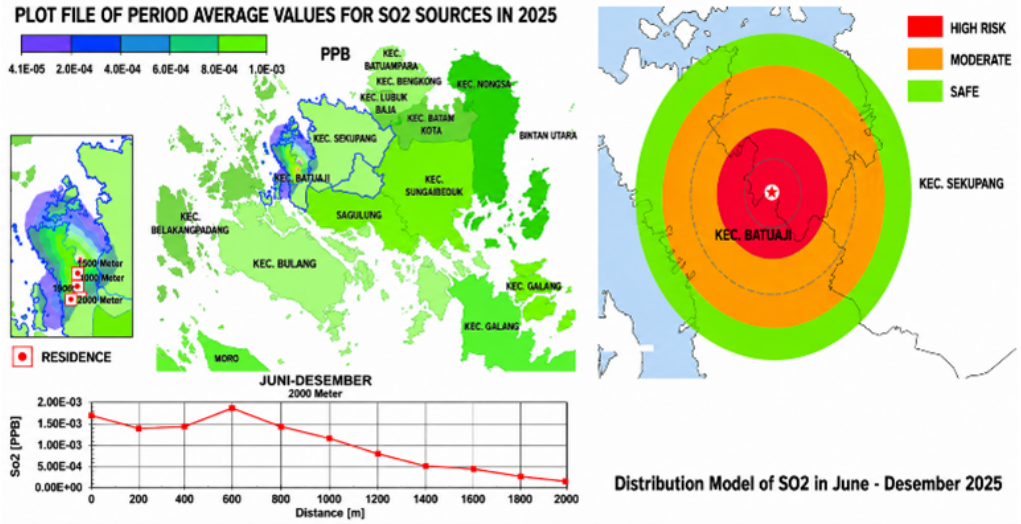

Figure 4. Concentration distribution modeling SO_2

Spatial analysis of SO_2 distribution showed a pattern of high concentrations around shipyard industrial estates, especially within a radius of 500–1000 m from emission sources. The red and orange colors on the map indicate zones with relatively high pollution levels that gradually decrease to yellow, green, and blue as the distance increases. This condition reflects the significant influence of industrial activities on the air quality in the surrounding area. The dispersion pattern tends to follow the dominant wind direction and local meteorological conditions, which are influenced by the topographic shape and structure of industrial buildings in the area.

The impact on settlements from the results of SO_2 distribution modeling shows that there are four main settlements within a radius of up to 2000 m from the shipbuilding industrial emission center that have the potential to be exposed to air pollution. The nearest settlement to the source of emissions is Renggam Citra Mas, which is located within a radius of approximately 500 m. This area is in the red to orange zone on the map, which reflects the highest SO_2 concentration. This suggests that people in the region face very high levels of exposure and the greatest health risks compared to other regions. In addition, Kampung Tua Cunting is located within a radius of approximately 1000 m from the source point. These areas are classified as orange to yellow zones, indicating high levels of exposure, although not as high as the closer areas. People in these areas are still at risk of being affected by long-term exposure, especially vulnerable groups such as children, the elderly, and those with asthma.

At a further radius of about 1500 m, there is the Pluto Residence. Based on the map, this area is in the greenish-yellow zone; Thus, the level of exposure can be categorized as moderate. Although lower than the previous two areas, the risk to health still needs to be considered, especially if exposure is continuous, while the farthest settlement that is still included in the zone of influence is the Ayana Tengah Public Housing located within a radius of 2000 m from the emission center.

The region is classified as a green zone on the map, reflecting a low level of exposure; However, the overall potential of pollutants in the long term remains a relevant issue for further study, especially if there are meteorological factors that slow the spread of clean air in the area. Overall, the order of exposure level from highest to lowest is Renggam Citra Mas, Kampung Tua Cunting, Pluto Housing, and Raya Ayana Pusat. This sequence is consistent with the distribution pattern of SO_2 concentrations, which are spread from industrial points as the main source of pollutants. The SO_2 concentration on the map is below the WHO daily threshold (20 μg/m^3 or ±7.6 ppb), but the cumulative and chronic nature of long-term exposure still poses a health risk that needs to be monitored [4]. In addition to its health impacts, SO_2 contributes to environmental pollution through the formation of acid rain, vegetation damage, soil quality degradation, and water pollution due to the deposition of compounds.

These results are supported by various previous studies that have linked residential distances to industrial emission sources and their impact on health. A study conducted in the Tanjung Uncang Batam shipyard industrial estate found that the concentration of SO_2 and particulate matter in the air around settlements within a radius of 1 km was above the national air quality standard threshold.

The study also reported an increase in respiratory complaints, such as chronic cough and shortness of breath, in exposed groups. The research [15] using the EMEP/EEA method found that industrial locations, including

shipyards, are the main source of SO_x emissions (including SO_2) in Batam based on the validity of the assumption that SO_2 comes from large industrial activities. From the theoretical approach and the results of the study, it can be explained that people who live within a radius of 500–1000 m from the shipyard are at the highest risk of health impacts due to SO_2 exposure. This pattern is in accordance with the basic principle of air pollution theory, that the intensity of exposure decreases as the distance from the source increases [16]. The results of the modeling and from previous research show that the order of exposure level from highest to lowest is Renggam Citra Mas, Kampung Tua Cunting, Pluto Housing, and Raya Ayana Pusat. This sequence is consistent with the principle of dispersion of pollutants distributed from the emission center, and the intensity decreases as the distance increases. The results of this study emphasize the importance of spatial planning and environmental supervision of industrial estates adjacent to settlements.

The spatial distribution of SO_2 concentrations was modeled using the AERMOD dispersion system in the shipyard area. The green contour lines represent zones where exposure to pollutants is minimal, expand outward from the emission source, and is influenced by local wind direction and land use patterns. The integration of receptor locations and residential areas allows for a clearer assessment of areas with negligible air pollution risks compared to the higher exposure zones presented in the previous figure.

3.3.3 Concentration distribution modeling NO_2

Figure 5 shows the distribution of NO_2 concentration in Batam City based on the results of measurements and spatial interpolation. This map shows the areas with the highest levels of exposure, which are generally around industrial areas.

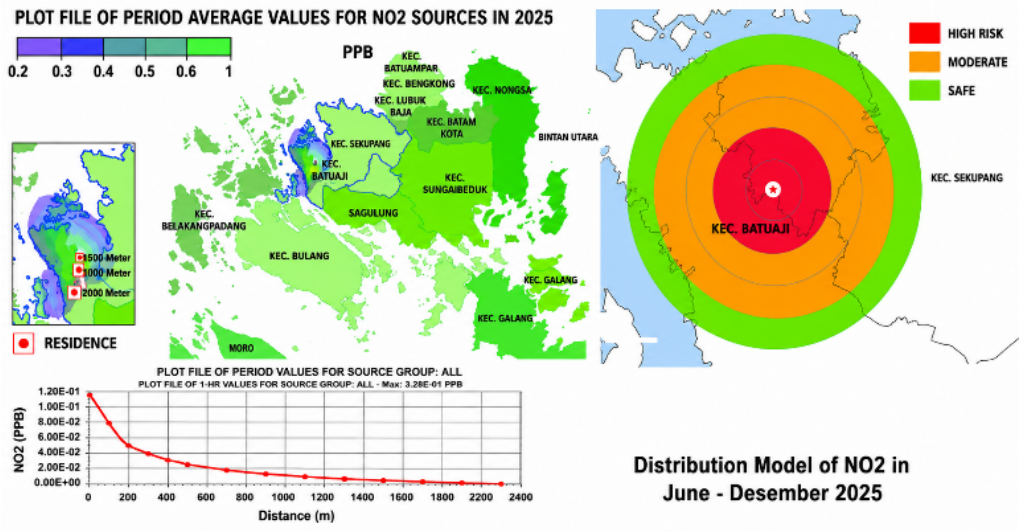

Figure 5. Concentration distribution modeling NO_2

The distribution map of NO_2 concentration below illustrates the spatial distribution of air quality in Batam City, especially around the shipyard industrial area. Data were obtained based on the results of field measurements and processed using spatial interpolation techniques to visualize the distribution pattern of NO_2 exposure. The colors on the map show a concentration gradient, where the red and orange areas mark the highest concentration, and the blue to purple areas indicate the lowest concentration. The highest concentrations were detected at points adjacent to industrial activities, indicating a significant influence from local emission sources. This information is important to understand the relationship between the intensity of industrial activities and potential health risks to the surrounding community.

Of the four settlement sites within a radius of $\leq$1000 m, NO_2 concentrations ranging from 25–40 ppb were in bright yellow and green areas, while settlements located in a radius of $>$1500 m showed relatively lower concentration values ($<$15 ppb), corresponding to the blue and purple color zones. The spatial distribution of NO_2 concentrations shown in the map is in line with the Gaussian Plume Model applied in the AERMOD simulation, which explains that the dispersion of pollutants follows a symmetrical bell-shaped curve, with the highest concentrations occurring at the central point of the emission source and decreasing exponentially in all directions according to prevailing wind patterns and other meteorological factors [16]. The application of AERMOD, which combines local meteorological parameters such as wind direction, temperature, and atmospheric stability [17]. According to the Regulation of the Minister of Environment and Forestry No. 14 of 2020, the annual ambient air quality standard for NO_2 is 53 ppb. Although the maximum values obtained in this study remained below this limit, continuous exposure in the range of

30–44 ppb has been associated with an increased risk of respiratory distress. Additionally, long-term exposure to NO_2 concentrations of 40 ppb or higher can adversely affect lung function, especially in vulnerable groups such as children, the elderly, and individuals with asthma [4].

The results of this study are strengthened by previous research; This study is in line with several previous study [17] that found concentrations of 35–47 ppb in shipyard areas in Semarang, especially in the dry season. According to the WHO [4], the main source of NO_2 exposure in the surrounding environment comes from the imperfect process of burning fossil fuels, NO_2 is one of the major polluting gases that belongs to the group of primary pollutants and at the same time is a precursor to secondary pollutants such as troposphere ozone and secondary particulate matter in the context of air pollution theories about the source of NO_2 exposure is important to explain the origin and dynamics of its existence in the atmosphere, anthropogenic sources are the largest contributor to NO_2 emissions, especially from industrial and transportation activities, including anthropogenic sources are the largest contributors to NO_2 emissions, especially from industrial and transportation activities including motor vehicle emissions, especially those using diesel and gasoline engines generates NO_2 through the oxidation reaction of nitrogen in the air during the combustion process. Heavy industries, including shipyards produce NO_2 from various processes such as the operation of diesel-fueled generator sets on sandblasting and welding activities that heat metals and the combustion process of paints and solvents that produce NO_2 as an initial product that oxidizes into NO_2 in the atmosphere. The main factor causing high NO_2 concentrations is the burning of fossil fuels from heavy equipment and industrial processes such as sandblasting, as described in a study [4].

Long-term exposure to NO_2 above 40 ppb may increase the risk of lung disease, especially in children and the elderly, as research conducted by Guo et al. [18] and Li et al. [19] also supported a correlation between NO_2 exposure and decreased lung function. These results corroborated that the maximum concentration of 44.2 ppb found in this study requires serious attention, although it is still below the national threshold. From an environmental health perspective, the WHO long-term exposure threshold for NO_2 is 10 μg/m^3 or the equivalent of ±5.3 ppb. Values on the map that exceed this threshold indicate that the region is in an unsafe zone and that people living in these zones are at risk of developing chronic respiratory diseases, such as asthma, chronic bronchitis, and decreased lung capacity [4].

3.3.4 Modeling the distribution of CO concentrations

The following modeling (Figure 6) shows the distribution of CO concentrations in Batam City based on the results of spatial and interpolation measurements, which reflect the dispersion pattern of pollutants from the main emission sources in the industrial area. The map shows that the areas with the highest levels of CO exposure are generally located around industrial areas, in line with the results of dispersion modelling using AERMOD software that takes into account the characteristics of emission sources and local meteorological conditions. Based on the Regulation of the Minister of Environment and Forestry Number P.14/MENLHK/SETJEN/KUM.1/7/2017 concerning the Air Pollutant Standard Index, the carbon monoxide threshold for 8 hours of exposure is set at 10,000 μg/m^3 (equivalent to ±8.7 ppm). The modeling results show that the maximum concentration of CO only reaches 16.9 ppb (±0.015 ppm), so it is still far below the national quality standard.

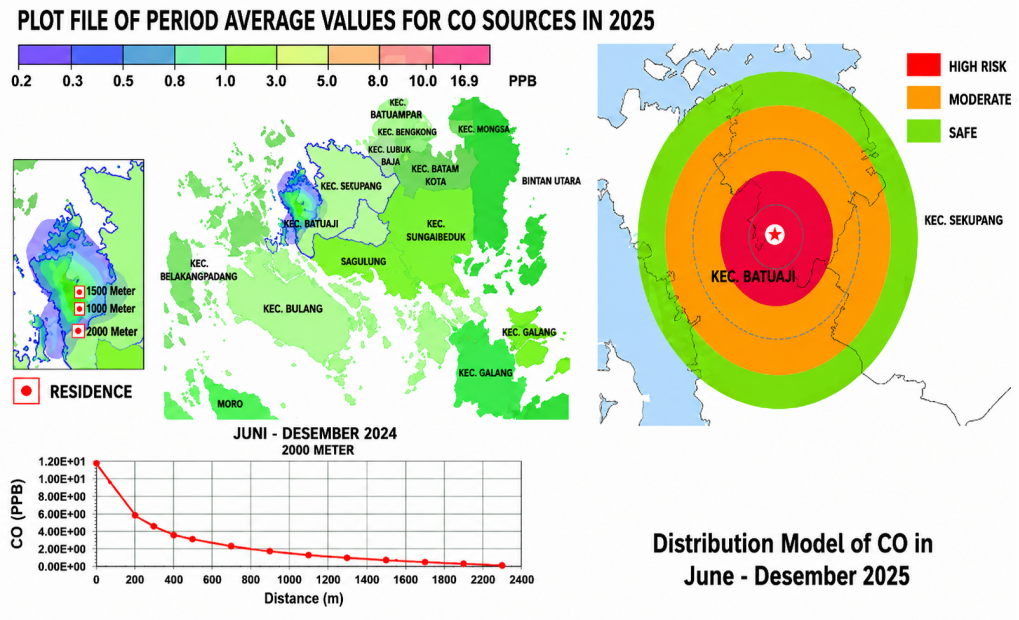

Figure 6. Modeling the distribution of CO concentrations

These findings are consistent with previous studies in industrial and coastal urban areas, which reported that CO concentrations are generally below regulatory thresholds, especially when emission sources are dominated by open industrial processes and transportation activities with relatively good levels of atmospheric dispersion. Previous studies have also shown that although CO concentrations are often low in absolute terms, their spatial distribution follows proximity to the emission source and is significantly influenced by wind direction and speed. Several AERMOD-based studies in heavy industrial estates and shipyards reported a similar pattern, where CO is diluted relatively faster than particulate pollutants, resulting in a slower concentration gradient as distance from the source increases.

Nevertheless, as reported in the literature, low concentration values do not necessarily negate health risks, especially in the context of long-term and cumulative exposure to populations living around industrial estates.

Exposure to chronic CO at low levels has been associated with impaired cardiovascular function and decreased blood oxygenation capacity, particularly in vulnerable groups such as children, the elderly, and individuals with respiratory or heart disease. Therefore, although the CO concentrations of these modeling results are well below quality standards, the integration of spatial analysis with health risk assessment is still necessary to understand the long-term implications of exposure in coastal urban industrial areas such as Batam City.

In addition, Government Regulation No. 22 of 2021 concerning the Implementation of Environmental Protection and Management highlights the importance of continuous air quality monitoring, especially in industrial estates near residential areas. Although CO concentrations have not exceeded established quality standards, the data suggest the need for strict precautions and monitoring to avoid potential increased emissions. Several previous studies have supported the importance of controlling air pollution from industrial activities. Previous studies have reported that air pollutant concentrations and their potential health impacts are influenced by proximity to emission sources as well as meteorological conditions that affect atmospheric dispersion and transport [20, 21]. These findings reinforce the fact that industrial activities, including shipyard operations, can elevate surrounding air pollutant concentrations and pose potential environmental risks; therefore, effective emission monitoring and control strategies are essential.

Figure 6 presents an environmental risk zoning map illustrating the distribution of air pollutant exposure levels in shipyard areas based on AERMOD dispersion modeling. The map depicts three risk categories: high, medium, and low risk, represented by red, orange, and green zones, respectively. These zones reflect the concentration gradient of pollutants originating from emission sources and are formed by local meteorological and topographic conditions. The integration of receptor points and residential areas provides a clear visualization of communities located within high-exposure zones, especially those located within or near high-risk contours. The map serves as a comprehensive tool for identifying priority areas for mitigation, air quality monitoring, and environmental health risk assessment.

3.3.5 Pb concentration distribution modeling

Figure 7 presents the spatial distribution of Pb concentration in Batam City derived from the results of measurement and interpolation. The map highlights the zones with the highest levels of exposure, especially in industrial areas.

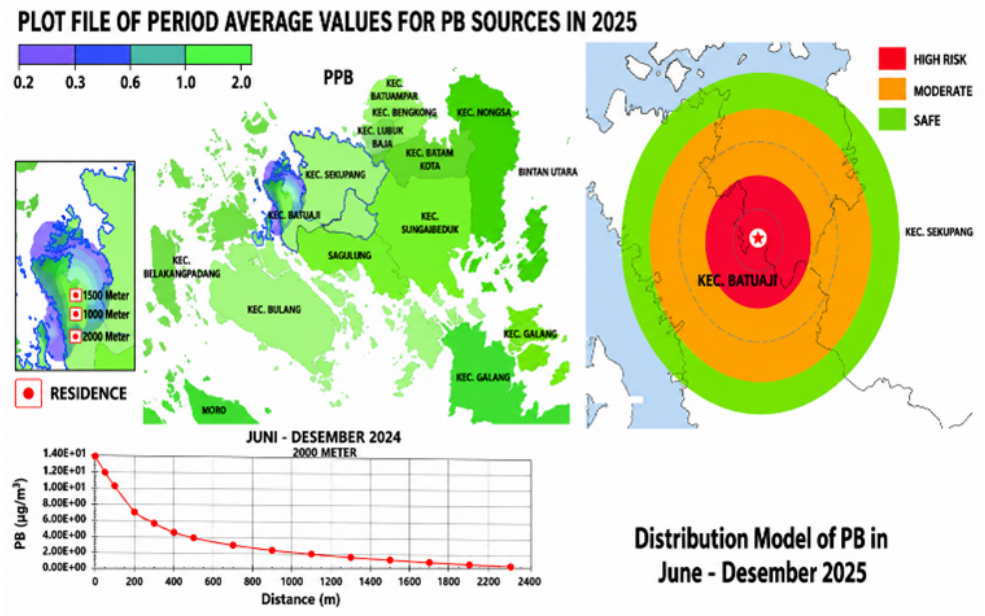

Figure 7. Concentration distribution modeling Pb

Based on Figure 7 of the distribution of Pb concentration modeling from AERMOD, it can be seen that the maximum value of Pb concentration reaches 2.16 $\mu g/m^3$ which is located at the coordinates (379885.29, 1186797.63), the area with the highest concentration is within a radius of less than 500 m from the source point, namely the shipyard industrial area which is strongly suspected to be the main source of lead emissions. The distribution pattern shows a configuration that conforms to the Gaussian blob dispersion principle, where the highest concentration is present around the source point and then decreases radially as the distance from the emission source increases. According to this theory, the distribution of pollutants in the atmosphere is strongly influenced by meteorological conditions (wind direction and speed), source characteristics (chimney height and emission rate), and local topography [22].

The map also shows the location of settlements within the radius of settlement distribution within a radius of $<$1000 m, such as Nagamas Citra Mas and Old Village Cunting, which are included in areas at high risk of exposure to Pb. The results of this study corroborate the results of a study [23], which examined the dispersion of heavy metal Pb in the Belawan Medan industrial estate, finding that the highest Pb concentration occurred within a radius of 500–700 m from the source of emissions of the port industry, and the concentration decreased as the distance from the source increased. The study also emphasizes that ship maintenance activities and the use of lead-based anti-corrosion paints are major contributors to air pollution. The study [8] examined the impact of the shipbuilding industry in Surabaya and found that the process of sandblasting and burning fossil fuels contributes significantly to the accumulation of Pb and other heavy metals in the surrounding air, especially during the dry season when particles are more easily suspended.

The distribution pattern of Pb concentrations in Batam, as depicted in this map, supports the previous results and shows that shipyard activities are the main source of air pollution by heavy metals, and residential areas within a radius of 0–1000 m are high-risk zones that require special attention in environmental and public health management. Therefore, integrated and ongoing mitigation efforts are needed to address this issue. The strategy involves implementing emission control technologies in industrial sources, strengthening environmental regulations and monitoring, establishing buffer zones between industrial and residential estates, raising public awareness of air pollution risks and self-protection measures, and conducting regular air quality monitoring with publicly accessible results. Active cooperation between government, industry, academia, and society is essential to minimize environmental risks and safeguard public health. This initiative is also in line with the principles of sustainable development outlined in the Sustainable Development Goals (SDGs) and the Regulation of the Minister of Environment and Forestry No. P.14/MENLHK/SETJEN/KUM.1/7/2017 on the environmental quality index.

These mitigation measures are also aligned with the SDGs, particularly SDG 3 (Good Health and Well-being), which emphasizes ensuring healthy living and promoting well-being for people of all ages; SDG 11 (Sustainable Cities and Communities), which focuses on the development of inclusive, safe, resilient, and sustainable urban areas; and SDG 13 (Climate Action), which calls for an urgent response to climate change and its impacts. Furthermore, air quality management is in accordance with national policies through the Regulation of the Minister of Environment and Forestry No. P.14/MENLHK/SETJEN/KUM.1/7/2017 concerning the Environmental Quality Index, which serves as a benchmark for assessing and improving environmental conditions at the regional level.

The resulting Environmental Risk Zoning uses AERMOD dispersion modeling to describe the spatial distribution of pollutant exposure around the shipyard area. The map classifies environmental risks into high-risk (red), medium-risk (orange), and low-risk (green) zones based on concentration gradients modeled from industrial emission sources. These zones reflect the influence of meteorological patterns, dominant wind direction, and surrounding land-use characteristics on the spread of pollutants. Overlays of receptor locations and residential areas allow for clear identification of communities located within high-exposure zones, especially those closest to emission sources. These maps provide an important basis for assessing potential health impacts, prioritizing mitigation measures, and guiding environmental management in affected areas.

3.3.6 Hazard Quotient of air pollutants at different receptor distances

Based on the results of the HQ assessment (Table 3 and Table 4), $PM_{2.5}$ showed the highest level of risk across the receptor distance, with HQ values ranging from 1.20 to 3.00, indicating significant non-carcinogenic health risks, especially in the 0–500 m zone. In contrast, NO_2, SO_2, CO, and Pb all showed HQ values of $<$1 across all receptor distances, indicating that exposure to these pollutants remains within acceptable limits. Overall, $PM_{2.5}$ was identified as the dominant pollutant that contributed the most to increased health risks in this study area.

Therefore, mitigation strategies should focus on controlling $PM_{2.5}$ as the primary pollutant through the application of covers, replacement of abrasive materials, scheduling of operations with minimal public exposure, installation of emission capture systems (local exhaust), and the implementation of regular air quality monitoring.

Table 5 presents the comparison between the $PM_{2.5}$ concentration field measurement results and the AERMOD simulation results, as well as the total emission load at various distances from the source. From the baseline, the baseline concentration and the total concentration (Baseline + Emission Burden) tend to decrease as the distance from the emission source increases.

Table 3. Hazard Quotient (HQ) of air pollutants at different receptor distances

Pollutant	Regulatory Standard (PP No.22/2021)	Distance (m)	Observed Concentration	HQ	Risk Classification
$PM_{2.5}$ ($\mu g/m^3$)	15.0	0–500	45	3.00	High risk (HQ $>$ 1)
		500–1000	35	2.33	High risk
		1000–1500	25	1.67	Moderate–High
		1500–2000	18	1.20	Moderate
SO_2 (ppb)	75	0–500	40	0.70	Acceptable
		500–1000	30	0.53	Acceptable
		1000–1500	20	0.35	Acceptable
		1500–2000	15	0.26	Acceptable
NO_2 (ppb)	50	0–500	50	1.00	Threshold
		500–1000	40	0.80	Moderate
		1000–1500	30	0.60	Low–Moderate
		1500–2000	25	0.50	Low
CO (ppm)	9	0–500	3.0	0.33	Acceptable
		500–1000	2.5	0.28	Acceptable
		1000–1500	2.0	0.22	Acceptable
		1500–2000	1.5	0.17	Acceptable
Pb ($\mu g/m^3$)	0.5	0–500	0.25	0.13	Acceptable
		500–1000	0.20	0.10	Acceptable
		1000–1500	0.15	0.08	Acceptable
		1500–2000	0.10	0.05	Acceptable

Table 4. Risk category (moderate Air Quality Index (AQI) based on Hazard Quotient (HQ))

Pollutant	Distance (m)	HQ	Risk Category (Moderate AQI)
$PM_{2.5}$ ($\mu g/m^3$)	0–500	3.00	High risk
	500–1000	2.33	High risk
	1000–1500	1.67	High risk
	1500–2000	1.20	High risk
SO_2 (ppb)	0–500	0.70	Acceptable
	500–1000	0.53	Acceptable
	1000–1500	0.35	Acceptable
	1500–2000	0.26	Acceptable
NO_2 (ppb)	0–500	0.47	Acceptable
	500–1000	0.38	Acceptable
	1000–1500	0.28	Acceptable
	1500–2000	0.24	Acceptable
CO (ppm)	All distances	0.1–0.33	Good
Pb ($\mu g/m^3$)	All distances	0.05–0.13	Acceptable

Table 5. Comparison of concentration of field measurement results and American Meteorological Society/Environmental Protection Agency Regulatory Model (AERMOD) simulation results for $PM_{2.5}$

Distance from Source (m)	Baseline Concentration ($\mu g/m^3$)	AERMOD Simulation Result ($\mu g/m^3$)	Baseline + Emission Load ($\mu g/m^3$)	Difference (Observed − Predicted)
500	45.17	3.47	48.64	41.70
1000	35.17	1.76	36.93	33.41
1500	25.33	0.242	25.57	25.09
2000	18.17	0.434	18.60	17.74
Average	**30.46**	**1.47**	**32.44**	**29.00**

At a distance of 500 m, the baseline concentration is 45.17 $\mu g/m^3$, while at 2000 m, it decreases to 18.17 $\mu g/m^3$. The results of the AERMOD simulation showed a relatively low additional emission load compared to baseline concentrations, ranging from 3.47 $\mu g/m^3$ (at 500 m) to 0.434 $\mu g/m^3$ (at 200 m). There is a significant difference between observed and predicted values after the addition of the emission burden. This difference is greatest at 500

m (41.70 μg/m^3) and decreases with distance, suggesting that the prediction model may be less accurate at shorter distances or that other conditions affect field measurements.

Table 6 shows the statistical validation between the observed field measurement results and the predicted AERMOD simulation results for $PM_{2.5}$, focusing on the difference squared value $(O-P)^2$. Based on the calculation results, R^2 = 0.95 was obtained, which indicates an excellent level of model conformity, as it conforms to the U.S. EPA criteria ($R^2 \geq 0.7$) for a statistically valid air dispersion model. The validation results between $PM_{2.5}$ concentrations from field measurements and AERMOD simulations showed a determination coefficient R^2 of 0.90. This value shows that the AERMOD model is able to explain about 90% of the variation in actual measurement data, so it can be categorized as having excellent predictive performance according to the U.S. EPA guidelines ($R^2 \geq 0.7$).

Table 6. Statistical validation between field measurement results and American Meteorological Society/Environmental Protection Agency Regulatory Model (AERMOD) simulation for $PM_{2.5}$

Distance from Source (m)	Observed (μg/m^3)	Predicted (μg/m^3)	$(O-P)^2$	R^2
500	45.17	3.47	1731.3	0.95
1000	35.17	1.76	1101.5	–
1500	25.33	0.242	632.7	–
2000	18.17	0.434	316.6	–
Average	**30.46**	**1.47**	–	–

Note: A dash (–) denotes no data.

However, the value of R^2 of 0.95 indicates a very strong linear relationship between the observed concentration and the model's predicted results. This high R^2 value indicates that AERMOD is able to capture the spatial trend of declining $PM_{2.5}$ concentrations as distances from emission sources increase, although in absolute terms the model still produces much lower concentration values.

The average $PM_{2.5}$ concentration from field measurements was 30.46 μg/m^3, while the average AERMOD prediction result was only 1.47 μg/m^3. This very striking difference indicates a systematic negative bias, where the model consistently underestimates $PM_{2.5}$ concentrations. This condition may be caused by several factors, including limited emission factor data, simplification of emission source characteristics (e.g., representation of area or volume sources), and failing to accommodate the contribution of other sources around the research site, such as traffic, port activities, and domestic sources. Overall, these results suggest that AERMOD is reliable in representing the spatial distribution pattern of $PM_{2.5}$, but still has limitations in reproducing the absolute concentration in the field. Therefore, it is necessary to improve input parameters and integrate more detailed field data so that the simulation results can be closer to actual conditions, especially for the purpose of environmental risk assessment and air pollution control policy making.

Table 7 shows the comparison between the baseline concentration, the results of the AERMOD simulation, and the total concentration, which is the sum of the two, at various distances from the emission source. The results of the analysis showed that the contribution of industrial emissions simulated using AERMOD to the concentration of SO_2 in ambient air was very small compared to the background concentration value.

Table 7. Comparison of the concentration of field measurement results and American Meteorological Society/Environmental Protection Agency Regulatory Model (AERMOD) simulation results for SO_2

Distance from Source (m)	Baseline Concentration (μg/m^3)	AERMOD Simulation Result (μg/m^3)	Baseline + Emission Load (μg/m^3)	Difference (Observed − Predicted)
500	40	0.0018	40.0018	39.9982
1000	30.17	0.0015	30.1715	30.1685
1500	20.17	0.00002	20.17002	20.16998
2000	15.17	0.00005	15.17005	15.16995
Average	**26.38**	**0.0018**	**26.38**	**26.00**

At a distance of 500 m from the emission source, the background concentration was recorded at 40 μg/m^3, while the contribution of the AERMOD simulation results was only 0.0018 μg/m^3. The addition of the emission load results in a total concentration of 40.0018 μg/m^3, which is practically no different from the background concentration. The same pattern was also observed at a distance of 1000 m to 2000 m, where the value of the AERMOD simulation results was in the range of 0.00002–0.0018 μg/m^3 and provided a very small increase in total concentration.

The difference between observed concentrations and observed–predicted concentrations that remained high over the entire observation distance indicated that the concentrations of $PM_{2.5}$ measured in the field were dominated

by background sources, not by the contribution of emissions from the modeled industrial sources. The average background concentration was 26.38 μg/m^3, while the contribution of the AERMOD simulation results was only 0.0018 μg/m^3, so the average difference reached about 26.00 μg/m^3.

These findings show that although AERMOD is able to simulate the dispersion of emissions from industrial sources, the average background NO_2 concentration is 36.29 μg/m^3, while the average contribution of the AERMOD simulation results is only 1.97 μg/m^3, resulting in an average total concentration of 37.76 μg/m^3. The average difference between the observed concentration and the predicted result of 34.33 μg/m^3 indicates that the contribution of industrial emissions to ambient NO_2 concentrations is relatively small compared to the pollutant load already present in the environment.

These findings suggest that NO_2 concentrations at the study site are most likely influenced by non-industrial sources, such as motor vehicle traffic, port activities, and regional transportation, which are not fully covered by the modeling scheme. Thus, although AERMOD is able to represent a pattern of decreasing industrial emission contribution to distance from source, this model tends to produce lower absolute concentration values than field measurements. Overall, the results in Table 8 confirm the importance of considering background concentrations and multiple sources of emissions in the interpretation of NO_2 modeling results. The integration between the results of the AERMOD simulation and the background concentration provides a more realistic picture of ambient air quality conditions as well as the relative role of industrial sources to NO_2 pollution in the study area.

Table 8. Comparison of the concentration of field measurement results and American Meteorological Society/Environmental Protection Agency Regulatory Model (AERMOD) simulation results for NO_2

Distance from Source (m)	Baseline Concentration (μg/m^3)	AERMOD Simulation Result (μg/m^3)	Baseline + Emission Load (μg/m^3)	Difference (Observed − Predicted)
500	50	3.33	53.33	46.67
1000	40	1.84	41.84	38.16
1500	30	0.255	30.255	29.745
2000	25.17	0.439	25.609	24.731
Average	**36.29**	**1.97**	**37.76**	**34.33**

Table 8 presents a comparison between NO_2 concentrations from field measurements, baseline concentrations, and AERMOD simulation results at various distances from emission sources. The results of the analysis showed that the ambient NO_2 concentration in the study area was dominated by background concentrations, while the contribution of emissions from the modeled industrial sources was relatively smaller, although it was still detected mainly at close proximity to the source.

At a distance of 500 m, the background concentration was recorded at 50 μg/m^3, while the AERMOD simulation result was 3.33 μg/m^3, so the total concentration increased to 53.33 μg/m^3. The contribution of industrial emissions at this distance is about 6%–7% of the background concentration, suggesting that the influence of emission sources is most pronounced in the near-field zone. However, as the distance from the source increases, the contribution of AERMOD decreases significantly due to the process of atmospheric dispersion, which is 1.84 μg/m^3 at a distance of 1000 m and less than 0.5 μg/m^3 at a distance of $\geq$1500 m.

Table 9 presents the statistical validation between the field measurement results (Observed) and the simulation results (Predicted) for NO_2 at the same distance. The results of the calculation of the R^2 value for NO_2 concentration showed that the AERMOD model was not able to adequately represent the field conditions. The R^2 value obtained is 0.94; the R^2 value of 0.94 indicates that approximately 94% of the observed NO_2 concentration variation can be explained by the results of the AERMOD simulation. This indicates a very strong linear relationship between the NO_2 concentration of field measurements and the modeling results of the distance from the emission source.

Table 9. Statistical validation between field measurement results and American Meteorological Society/Environmental Protection Agency Regulatory Model (AERMOD) simulation for NO_2

Distance from Source (m)	Observed (μg/m^3)	Predicted (μg/m^3)	$(O-P)^2$	R^2
500	50	3.33	46.67	0.94
1000	40	1.84	38.16	–
1500	30	0.255	29.745	–
2000	25.17	0.439	24.731	–
Average	**36.29**	**1.97**	–	–

Note: A dash (–) denotes no data.

Nevertheless, despite the high R^2 value, the results of the AERMOD simulation still show a considerable underestimation of the absolute NO_2 concentration, especially at close proximity to the source. This condition confirms that AERMOD is able to represent the spatial pattern of NO_2 distribution, but still has limitations in predicting the actual concentration in the field.

Table 10 presents a comparison between CO concentrations from field measurements and AERMOD simulation results at four receptor distances. The baseline concentration decreased consistently with increasing distance from the emission source, ranging from 3.05 μg/m^3 at 500 m to 1.52 μg/m^3 at 2000 m, with an average of 2.285 μg/m^3. The AERMOD simulation results were generally lower than the field measurements, ranging from 3.19 μg/m^3 at 500 m to 0.445 μg/m^3 at 2000 m, with an average of 1.372 μg/m^3. The total concentration (Baseline + Emission Load) ranged from 6.24 μg/m^3 at 500 m to 1.965 μg/m^3 at 2000 m, with an average of 3.657 μg/m^3. The difference between observed and predicted values (Observed − Predicted) was -0.14 at 500 m, indicating slight overestimation by the model at this distance, while positive differences of 0.96, 1.76, and 1.07 were recorded at 1000, 1500, and 2000 m respectively, suggesting underestimation at greater distances. The largest discrepancy occurred at 1500 m (1.76 μg/m^3), which represents the point of greatest deviation between model prediction and field measurement.

Table 10. Comparison of the concentration of field measurement results and American Meteorological Society/Environmental Protection Agency Regulatory Model (AERMOD) simulation results for CO

Distance from Source (m)	Baseline Concentration (μg/m^3)	AERMOD Simulation Result (μg/m^3)	Baseline + Emission Load (μg/m^3)	Difference (Observed − Predicted)
500	3.05	3.19	6.24	-0.14
1000	2.55	1.59	4.14	0.96
1500	2.02	0.261	2.281	1.76
2000	1.52	0.445	1.965	1.07
Average	**2.285**	**1.372**	**3.657**	**0.91**

Table 11 shows the comparisons between CO concentrations from field measurements and AERMOD predictions show that models tend to estimate lower values than observations, especially at distances of 1500 and 2000 m. However, the pattern of concentration decline as distance from sources increased remained consistent across both datasets, suggesting that AERMOD was able to represent pollutant dispersion trends well. The square value of the $(O - P)^2$ difference indicates the degree of deviation of the model, with the highest value at a distance of 1500 m, which is the point with the greatest difference between the prediction and the measurement.

Table 11. Statistical validation between field measurement results and American Meteorological Society/Environmental Protection Agency Regulatory Model (AERMOD) simulation for CO

Distance from Source (m)	Observed (μg/m^3)	Predicted (μg/m^3)	$(O - P)^2$	R^2
500	3.05	3.19	0.0196	0.84
1000	2.55	1.59	0.8836	–
1500	2.02	0.261	3.0820	–
2000	1.52	0.445	1.1540	–
Average	–	–	**1.285**	–

Note: A dash (–) denotes no data.

The value R^2 = 0.84 indicates that approximately 84% of the variation in CO concentration results from field measurements can be explained by the results of the AERMOD simulation. Based on model evaluation practices that refer to the U.S. EPA and supporting literature, these values fall into the category of excellent relationships.

These results indicate that AERMOD is very capable of representing the spatial pattern of CO distribution at distances from the emission source. Compared to the other pollutants in the study, CO showed the most consistent model performance, characterized by relatively small $(O - P)^2$ values at close quarters as well as high R^2 values. Despite the increase in the difference in medium to long distances, the value of R^2 = 0.84 showed a very strong linear relationship between the CO concentration measured and the AERMOD simulation results. This high R^2 value indicates that AERMOD is able to consistently capture the spatial pattern of declining CO concentrations over distances from emission sources.

Table 12 presents a comparison between the Pb concentration from field measurements at various distances with the reference values set in Government Regulation Number 22 of 2021. In general, Pb concentrations show a decreasing pattern as the distance from the emission source increases. At a distance of 500 meters, the concentration of Pb was recorded at 0.25 μg/m^3, then decreased to 0.20 μg/m^3 at 1000 meters, 0.15 μg/m^3 at 1500 meters, and

reached a low value of 0.10 μg/m^3 at a distance of 2000 meters from the source. When compared to the national quality standard of 0.50 μg/m^3, all measurement results were well below the reference value. This can be seen from the negative difference between the observed concentration and the predicted/reference value, which ranges from -0.40 to -0.25 μg/m^3. These results show that despite industrial activity around the monitoring site, the Pb load in the surrounding air is still at a relatively safe level and does not exceed the maximum permissible limit value. When the base value is combined with the baseline value (Baseline + Emission Load), it can be seen that the highest theoretical concentration is 0.75 μg/m^3 at a distance of 500 meters, and the lowest is 0.60 μg/m^3 at 2000 meters. Although this value only illustrates the potential for increased pollutant loads, the table shows that the contribution of emissions from sources still needs to be further analyzed to understand their potential for ambient air quality.

Table 12. Comparison of the concentration of field measurement results and American Meteorological Society/Environmental Protection Agency Regulatory Model (AERMOD) simulation results for Pb

Distance from Source (m)	Baseline Concentration (μg/m^3)	AERMOD Simulation Result (μg/m^3)	Baseline + Emission Load (μg/m^3)	Difference (Observed − Predicted)
500	0.25	0.50	0.75	-0.25
1000	0.20	0.50	0.70	-0.30
1500	0.15	0.50	0.65	-0.35
2000	0.10	0.50	0.60	-0.40
Average	**0.175**	**0.50**	**0.675**	**-0.33**

Table 13 presents the results of statistical validation between the Pb concentrations of field measurements and the results of AERMOD simulations at various distances from emission sources. In general, the results of the analysis show a very good degree of compatibility between the observed value and the prediction result, both in terms of concentration and spatial distribution pattern.

Table 13. Statistical validation between field measurement results and American Meteorological Society/Environmental Protection Agency Regulatory Model (AERMOD) simulation for Pb

Distance from Source (m)	Observed (μg/m^3)	Predicted (μg/m^3)	$(O-P)^2$	R^2
500	0.25	0.30	0.0025	0.94
1000	0.20	0.18	0.0004	–
1500	0.15	0.12	0.0009	–
2000	0.10	0.08	0.0004	–
Average	–	–	**0.00105**	–

Note: A dash (–) denotes no data.

At a distance of 500 m, the Pb concentration was observed to be 0.25 μg/m^3, while the AERMOD simulation results were 0.30 μg/m^3, with a very small value $(O-P)^2$ (0.0025). A similar pattern of conformity was also seen at distances of 1000 m to 2000 m, where values $(O-P)^2$ were in the range of 0.0004–0.0009. This low squared error value indicates that the deviation between the measurement results and the simulation results is relatively minimal over the entire observation distance.

The mean value $(O-P)^2$ of 0.00105 reflects a very low overall CO prediction error rate. In addition, the value of R^2 = 0.94 indicates a very strong linear relationship between the Pb concentration of the field measurements and the results of the AERMOD simulation. This shows that AERMOD is not only able to capture the downward trend of Pb concentrations relative to the distance from the emission source, but also quite accurately represents the absolute concentration amount. Compared to other pollutants analyzed in this study, such as $PM_{2.5}$, SO_2, and NO_2, AERMOD's performance in modeling Pb is classified as the most consistent and reliable. This is likely due to the relatively stable characteristics of Pb emissions as well as the dispersion process in the atmosphere, which is more in line with the basic assumptions of the AERMOD model.

Overall, the results in Table 13 confirm that AERMOD has an excellent performance in modeling Pb concentrations in the study area, making it reliable for the evaluation of the spatial distribution and contribution of Pb emissions from industrial sources.

The results of AERMOD's performance evaluation showed that there was a clear difference in performance between pollutants, both in terms of absolute value conformity and prediction error rate. For Pb, the model showed the best performance, characterized by a very low error value and a high coefficient of determination (R^2 = 0.84–0.94), which indicates that AERMOD is able to accurately represent both spatial patterns andPb concentration quantities. In contrast, for $PM_{2.5}$, SO_2, and NO_2, although the R^2 value was also high (>0.90) and showed a strong spatial

distribution pattern, the simulation results consistently underestimated the absolute concentration compared to field measurements.

The inconsistency of the model's performance between pollutants suggests that AERMOD's main limitation in this study lies not in the model's ability to capture dispersion trends, but rather in the parameterization of emission sources and the dominance of different background concentrations for each pollutant. $PM_{2.5}$ and NO_2 are strongly influenced by non-industrial sources such as regional traffic and transportation, while SO_2 shows high sensitivity to the accuracy of emission factors and source characteristics. Thus, differences in model performance reflect the physical–chemical characteristics of pollutants and the complexity of emission sources, rather than general model failures. These findings confirm that the evaluation of AERMOD's performance needs to be carried out on a pollutant-specific basis, as well as integrating background concentrations and multiple emission sources to obtain a more accurate and fair interpretation of the model's performance.

Although some pollutants remain below regulatory concentration thresholds, HQ analysis shows that $PM_{2.5}$ poses a significant non-carcinogenic health risk, with HQ values exceeding unity at all receptor distances. These results illustrate that health risks are not only determined by adherence to ambient air quality standards, but also by cumulative exposure and toxicological sensitivity. $PM_{2.5}$ exhibits a disproportionate health risk due to its ability to penetrate deep into the respiratory tract, even at relatively low environmental concentrations. In contrast, SO_2, CO, and Pb present acceptable HQ values, while NO_2 approaches the risk threshold level at closer distances, indicating potential concern for sensitive populations. These findings reinforce the need to integrate spatial exposure analysis with health risk metrics to capture the full coverage of environmental health impacts in industrial coastal environments.

Overall, the integration of multi-pollutant spatial dispersion modeling with health risk assessment provides a comprehensive framework for understanding the environmental impacts of shipbuilding industrial activities. By simultaneously examining concentration gradients, spatial distribution patterns, and health risk indexes, the study moves beyond purely technical evaluation of air quality and elucidates the spatial relationship between emission sources and population exposure. These findings suggest that environmental risks are not only shaped by the level of pollutant concentrations but also by spatial persistence, dispersion behavior, and proximity to residential receptors. This integrated perspective offers applied insights that can be generalized to other coastal industrial estates with similar emission characteristics, supporting more informed environmental management and public health protection strategies.

4 Conclusion

This study provides strong empirical evidence that shipyard industrial activities in the coastal area of Batam City have a significant effect on ambient air quality and non-carcinogenic health risks of the surrounding community. The results of field measurements show a consistent spatial gradient, where the concentration of pollutants decreases as the distance from the emission source increases. Among the pollutants studied, $PM_{2.5}$ was identified as a major risk factor because it exhibited a high relative concentration and a HQ value of >1 at the entire receptor distance, specifically within a radius of 0–2000 m from the source. Meanwhile, NO_2, SO_2, CO, and Pb all fall within the acceptable risk category across all receptor distances, indicating no significant non-carcinogenic health risk from these pollutants.

A comparison between the results of direct measurements and the AERMOD simulation shows that the model is able to represent the spatial dispersion pattern and the downward trend of concentration at distances well, as indicated by the high value of the determination coefficient ($R^2 > 0.84$). However, the model systematically tends to underestimate the absolute concentration amount, particularly for $PM_{2.5}$, SO_2, and NO_2, which indicates a significant influence of background concentrations as well as the contribution of non-industrial emission sources that have not been fully accommodated in the model parameterization. Nonetheless, AERMOD's strength in capturing spatial distribution patterns makes it reliable for region-based exposure analysis.

Overall, the integration of air quality measurement, multi-pollutant dispersion modeling, and health risk assessment provides a more comprehensive analytical framework than the evaluation of quality standard compliance alone. This approach confirms that environmental health risks are determined not only by the level of pollutant concentrations but also by spatial persistence, toxicological characteristics, and proximity to settlements. These findings have important implications for the formulation of air pollution control policies, industrial spatial planning, and public health protection strategies in coastal industrial estates with similar characteristics.

Author Contributions

Conceptualization, A.P.; methodology, A.P.; software, A.P.; investigation, A.P.; data curation, A.P.; formal analysis, A.P.; writing—original draft preparation, A.P.; writing—review & editing, A.P., B.A., A.A., and B.B.; supervision, B.A. All authors have read and agreed to the published version of the manuscript.

Data Availability

The data used to support the findings of this study are available from the corresponding author upon request.

Acknowledgment

The authors would like to thank Ibnu Sina University for all the facilities, financial support, and assistance provided during the research. The authors would also like to express their deepest gratitude and appreciation to all parties involved in the completion of this research and publication.

Conflicts of Interest

The authors declare no conflicts of interest.

References

[1] M. P. Todaro and S. C. Smith, *Economic Development (12th Edition)*. New York: Pearson Education, 2015.

[2] Ministry of Environment and Forestry of the Republic of Indonesia, "Peraturan Menteri Lingkungan Hidup dan Kehutanan Nomor 14 Tahun 2020 tentang Indeks Standar Pencemar Udara," 2020. https://peraturan.bpk.go.id/Details/163466/permen-lhk-no-14-tahun-2020

[3] S. Maji, S. Ahmed, M. Kaur-Sidhu, S. Mor, and K. Ravindra, "Health risks of major air pollutants, their drivers and mitigation strategies: A review," *Air Soil Water Res.*, vol. 16, p. 117862212311546, 2023. https://doi.org/10.1177/11786221231154659

[4] World Health Organization, *WHO Global Air Quality Guidelines: Particulate Matter ($PM_{2.5}$ and PM_{10}), Ozone, Nitrogen Dioxide, Sulfur Dioxide, and Carbon Monoxide*. World Health Organization, 2021.

[5] T. Y. Su, C. H. Pan, Y. T. Hsu, W. F. Li, and C. H. Lai, "Effects of heavy metal exposure on shipyard welders: A cautionary note for 8-hydroxy-2'-deoxyguanosine," *Int. J. Environ. Res. Public Health*, vol. 16, no. 23, p. 4813, 2019. https://doi.org/10.3390/ijerph16234813

[6] H. M. Tran, C. H. Lai, W. L. Chen, C. C. Wang, C. W. Liang, C. Y. Chien, C. H. Pan, K. J. Chuang, and H. C. Chuang, "Effects of occupational exposure to metal fume $PM_{2.5}$ on lung function and biomarkers among shipyard workers: A 3-year prospective cohort study," *Int. Arch. Occup. Environ. Health*, vol. 97, no. 4, pp. 401–412, 2024. https://doi.org/10.1007/s00420-024-02055-1

[7] T. Hoek, R. Beelen, K. de Hoogh, D. Vienneau, J. Gulliver, P. Fischer, and D. Briggs, "A review of land-use regression models to assess spatial variation of outdoor air pollution," *Atmos. Environ.*, vol. 42, no. 33, pp. 7561–7578, 2008. https://doi.org/10.1016/j.atmosenv.2008.05.057

[8] M. Jerrett, A. Arain, P. Kanaroglou, B. Beckerman, D. Potoglou, T. Sahsuvaroglu, J. Morrison, and C. Giovis, "A review and evaluation of intraurban air pollution exposure models," *J. Exposure Anal. Environ. Epidemiol.*, vol. 15, no. 2, pp. 185–204, 2005. https://doi.org/10.1038/sj.jea.7500388

[9] B. Kura, A. K. Hussein, and M. S. Mohd Najib, "Atmospheric particulate emissions from dry abrasive blasting," *J. Air Waste Manage. Assoc.*, vol. 56, no. 11, pp. 1559–1567, 2006. https://doi.org/10.1080/10473289.2006.10464533

[10] F. Karagulian, C. A. Belis, C. F. C. Dora, A. M. Prüss-Ustün, S. Bonjour, H. Adair-Rohani, and M. Amann, "Contributions to cities' ambient particulate matter (PM): A systematic review of local source contributions at the global level," *Atmos. Environ.*, vol. 120, pp. 475–483, 2015. https://doi.org/10.1016/j.atmosenv.2015.08.087

[11] J. M. Mazurek and M. D. Attfield, "Silicosis mortality among young adults in the United States, 1968–2004," *Am. J. Ind. Med.*, vol. 51, no. 8, pp. 568–578, 2008. https://doi.org/10.1002/ajim.20597

[12] C. C. Leung, I. T. S. Yu, and W. Chen, "Silicosis," *Lancet*, vol. 379, no. 9830, pp. 2008–2018, 2012. https://doi.org/10.1016/S0140-6736(12)60235-9

[13] C. Guo, G. Hoek, L. Y. Chang, Y. Bo, C. Lin, B. Huang, T. C. Chan, T. Tam, A. K. H. Lau, and X. Q. Lao, "Long-term exposure to ambient fine particulate matter ($PM_{2.5}$) and lung function in children, adolescents, and young adults: A longitudinal cohort study," *Environ. Health Perspect.*, vol. 127, no. 12, p. 127008, 2019. https://doi.org/10.1289/EHP5220

[14] Y. Guan, Y. Xiao, B. Li, and N. Zhang, "Measuring the synergy of air pollution and CO_2 emission in Chinese urban agglomerations: An evaluation from the aggregate impact and correlation perspectives," *Stoch. Environ. Res. Risk Assess.*, vol. 38, no. 7, pp. 2693–2709, 2024. https://doi.org/10.1007/s00477-024-02705-3

[15] A. Triwinarko, D. Kartikasari, D. Istardi, S. Ghozali, and D. Mulyaningtyas, "Air pollutant emissions in Batam: An overview," *J. Teknol.*, vol. 77, no. 23, 2015. https://doi.org/10.11113/jt.v77.6692

[16] D. B. Turner, *Workbook of Atmospheric Dispersion Estimates: An Introduction to Dispersion Modeling*. CRC Press, 2020.

[17] U.S. Environmental Protection Agency (EPA), "Air Quality Dispersion Modeling—Preferred and Recommended Models," 2023. https://www.epa.gov/scram/air-quality-dispersion-modeling-preferred-and-recommended-models

[18] J. Z. Guo, Y. P. Chen, W. D. Zhang, S. Tong, and J. G. Dong, "Moderate and severe exacerbations have a significant impact on health-related quality of life, utility, and lung function in patients with chronic obstructive pulmonary disease: A meta-analysis," *Int. J. Surg.*, vol. 78, pp. 28–35, 2020. https://doi.org/10.1097/JS9.0000000000001448

[19] Z. Li, X. Bao, Y. Sheng, and Y. Xia, "Research on unsafe behavior of construction workers under the bidirectional effect of formal rule awareness and conformity mentality," *Front. Psychol.*, vol. 12, p. 794394, 2021. https://doi.org/10.3389/fpsyg.2021.794394

[20] D. W. Dockery and C. A. Pope III, "Acute respiratory effects of particulate air pollution," *Annu. Rev. Public Health*, vol. 15, pp. 107–132, 1994. https://doi.org/10.1146/annurev.pu.15.050194.000543

[21] A. P. K. Tai, L. J. Mickley, and D. J. Jacob, "Correlations between fine particulate matter ($PM_{2.5}$) and meteorological variables in the United States: Implications for the sensitivity of $PM_{2.5}$ to climate change," *Atmos. Environ.*, vol. 44, no. 32, pp. 3976–3984, 2010. https://doi.org/10.1016/j.atmosenv.2010.06.060

[22] J. H. Seinfeld and S. N. Pandis, *Atmospheric Chemistry and Physics: From Air Pollution to Climate Change*. John Wiley & Sons, 2016.

[23] F. Meilasari, H. Sutrisno, and B. Purwoko, "Analisis sebaran lindi di sekitar kawasan TPA Batu Layang berdasarkan nilai resistivitas," *J. Teknol. Lingkung.*, vol. 24, no. 1, pp. 10–20, 2023. https://doi.org/10.55981/jtl.2023.247